

Pyrolytically grown arrays of highly aligned $B_xC_yN_z$ nanotubes

Wei-Qiang Han, John Cumings, and Alex Zettl^{a)}

Department of Physics, University of California, Berkeley, California 94720, and Materials Science Division, Lawrence Berkeley National Laboratory, Berkeley, California 94720

(Received 12 December 2000; accepted for publication 5 March 2001)

A pyrolysis route has been used to synthesize arrays of highly aligned $B_xC_yN_z$ nanotubes in bulk. The structure and composition of the product were characterized by scanning electron microscopy, high-resolution transmission electron microscopy, and electron energy-loss spectroscopy. The length and diameter of the nanotubes are quite uniform in a large area of the reaction zone. The sizes of the aligned $B_xC_yN_z$ nanotubes from the whole reaction zone are 10–30 μm in length and 20–140 nm in diameter. The x/z ratio of $B_xC_yN_z$ nanotubes for most nanotubes is about 1:1. The x/y ratio of $B_xC_yN_z$ nanotubes is up to 0.6. Within one nanotube, the x/y ratio is usually heterogeneous. The growth mechanism is also discussed. © 2001 American Institute of Physics.
[DOI: 10.1063/1.1369620]

Pure carbon nanotubes show a variety of electronic behaviors from metallic to semiconducting, depending on composition, chirality, and diameter.¹ However, the systematic application of these varied electronic properties is presently difficult. Synthesis of B- and/or N-substituted nanotubes is possibly one method to control the electronic properties of nanotubes in a well-defined way. The experimental verification of the existence and the electronic properties of such hetero nanotubes is a topic of current research.^{2–14} Among the possible applications, $B_xC_yN_z$ nanotubes are predicted as possible candidates for nanosized electronic and photonic device with a large variety of electronic properties since these nanotubes are energetically stable.³

Alignment of nanotubes is important to enable both fundamental studies and applications, such as scanning probes, sensors, cold cathode flat panel displays, and nanoelectronics. Recently, Shelimov *et al.*¹⁵ reported the formation of BN nanotubules arrays by pyrolyzing 2-, 4-, 6-trichloroborazine over porous anodic alumina templates and coaxial C/BN/C nanotubes arrays by the sequential pyrolysis of acetylene and trichloroborazine over alumina templates. However, the diameter ranges from 270 to 360 nm and the wall thickness is about 110 nm. Recently, Bai *et al.*¹⁶ have reported the formation of aligned B–C–N nanotubes, which show blue-violet photoluminescence, by bias-assisted hot filament chemical vapor deposition from the source gases of B_2H_6 , CH_4 , N_2 , and H_2 . The diameters of these nanotubes are again very large and range from 50–260 nm. Pyrolysis of organometallic precursors such as metallocenes and iron pentacarbonyl have been carried out under a variety of conditions to synthesize aligned carbon and aligned nitrogen doped carbon nanotubes.^{11,13,14,17–19}

In the present study, we describe the use of a pyrolysis route which combines pyrolyzation of a mixture of ferrocene and melamine and vaporization of molten boron oxide under ammonia atmosphere for large scale fabrication of arrays of highly aligned $B_xC_yN_z$ nanotubes with uniform length and

small diameter. Uniform aligned nanotubes with thin diameter have great advantages for possible applications, such as field emission.

In order to prepare the aligned $B_xC_yN_z$ nanotube arrays, a two-stage furnace system fitted with temperature controllers was employed.^{7,14} The flow rate of gases was controlled by using mass flow controllers. A (1:2:0.2) mixture (by weight) of powdered ferrocene [bis(cyclopentadienyl)iron, $(C_5H_5)_2Fe$, Aldrich 98%], melamine ($C_3H_6N_6$, Fluka 99%) and boron oxide (B_2O_3 , 99.99%) was divided into two equal portions and placed side by side in a quartz tube (inner diameter 9 mm). The furnace was set to 1050 °C with ammonia flowing through the tube at 20–30 sccm. The quartz tube was placed so that one portion was inside the furnace and the other was upstream, outside the furnace. After 3 min, the flow rate was increased to 100 sccm in order to blow the second portion into the furnace. The flow rate was then reduced to 20–30 sccm again, and the temperature was increased rapidly to 1150 °C and maintained for 15–20 min. The system was then allowed to cool to room temperature and soot-like deposits were collected from the quartz tube. The resulting sample was characterized by scanning electron microscopy (SEM) using a JEOL JSM-6340 field emission microscope, high-resolution transmission electron microscopy (HRTEM) using a Philips CM200 FEG equipped with a parallel electron energy-loss spectroscopy detector (EELS, Gatan PEELS 678).

To reveal the growth process of the aligned nanotubes, SEM was used to examine the general morphology. In Figs. 1(a) and 1(b), we show the typical SEM images of the aligned nanotubes. The low magnification image in Fig. 1(a) shows bundles of highly aligned nanotubes. The length and diameter of the nanotubes are quite uniform in a large area of the reaction zone. The sizes of the aligned $B_xC_yN_z$ nanotubes from the whole reaction zone are 10–30 μm in length and 20–140 nm in diameter. In preparation for SEM, the nanotube material naturally breaks along the direction of the aligned nanotubes. The high magnification image in Fig. 1(b) clearly reveals a high density of aligned nanotubes at the edge of one of these fractures.

^{a)}Author to whom correspondence should be addressed; electronic mail: azettl@physics.berkeley.edu

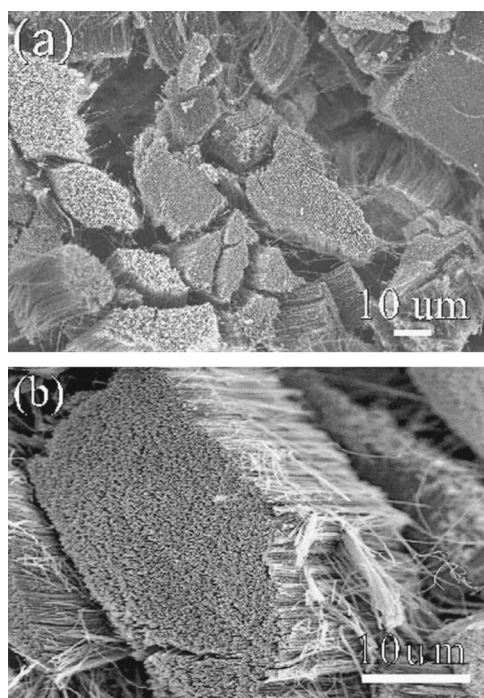


FIG. 1. (a) Low magnification SEM image showing a general view of the bundles of the aligned $B_xC_yN_z$ nanotubes and (b) high magnification SEM micrograph revealing a high density of aligned nanotubes.

TEM investigation shows the nanotubes possess irregular bamboo-like morphologies with wide core diameters as shown in Fig. 2(a). HRTEM reveals that the thin tube walls are composed of graphitic layers, which make up the stacked bamboo-like tubules [Fig. 2(b)]. The interplanar spacing of nanotubes is ~ 0.34 nm. The microstructure of these aligned nanotubes is similar to that of aligned CN_x nanotubes reported elsewhere.¹⁴ Iron nanoparticles are frequently found in the tip of nanotubes.

EELS characterizations of the K -edge absorption for boron, carbon, and nitrogen were used to estimate the stoichiometry of the nanotubes. Spectra were obtained using about 5–10 nm probes. A typical EELS spectrum from an individual nanotube is shown in Fig. 3(a). Three distinct absorption features are revealed, starting from 188, 284, and 403 eV, corresponding to the known B- K , C- K , and N- K edges, respectively. The B/C and N/B atomic ratios of the nanotube were 0.55 and 0.90, respectively. Figure 3(b) shows EELS spectra recorded at four locations along the nanotube shown in Fig. 2(a). The spectrum at the tip is labeled a, and the other spectra along the tube are labeled b, c, and d. EELS measurements reveal that the B/C and N/C atomic ratios are 0.40 and 0.37 in a. The B/C and N/C atomic ratios in b, c, and d are 0.26–0.18, 0.38–0.26, and 0.23–0.23, respectively. The heterogeneous composition within a nanotube could be caused by the nonuniform atmosphere around the growth region of nanotubes. Taking into consideration the experimental error of about 10% due mainly to background subtraction when the EELS spectra are analyzed, the x/z ratio of $B_xC_yN_z$ nanotubes for most nanotubes is about 1:1. This suggests that B and N radicals prefer to incorporate into the network of the nanotubes in the ratio of 1:1. The x/y ratio of $B_xC_yN_z$ nanotubes is up to 0.6.

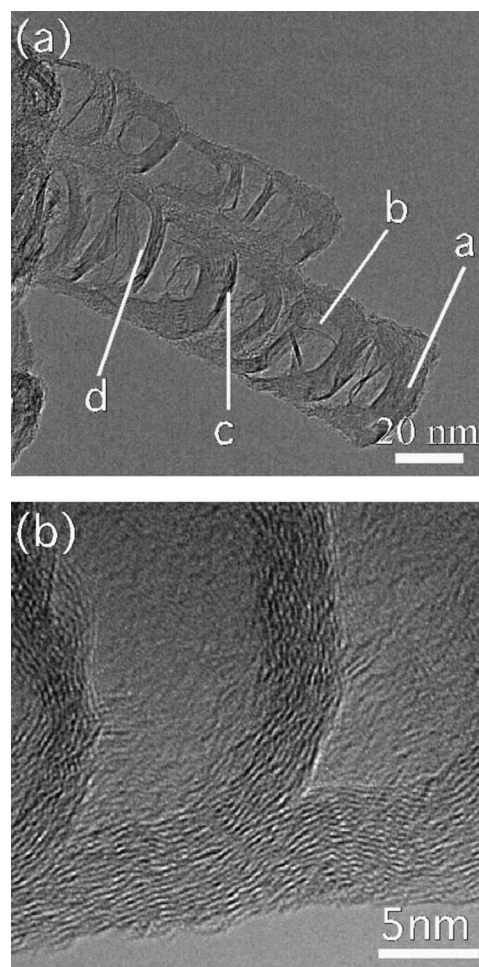


FIG. 2. (a) TEM image showing the nanotubes possess irregular bamboo-like morphologies with wide core diameters. Labels a, b, c, and d are four locations along a nanotube where EELS spectra were recorded and (b) HRTEM reveals that the thin tube walls are composed of graphitic layers, which make up the stacked bamboo-like tubules.

Around 20% of the nanotubes contain the x/y ratio of higher than 0.01.

Omission of ferrocene in our initial pyrolysis experiment results in no nanotubes in the product, which supports the crucial catalytic role of ferrocene. Omission of melamine in our initial pyrolysis experiment results in the formation of aligned nanotubes, but the x/y ratio is less than that of our initial aligned $B_xC_yN_z$ nanotubes. This suggests melamine, which thermally decomposes into CN radicals at high temperature, plays an important role for the synthesis of high quality $B_xC_yN_z$ nanotubes. Control experiments with the same experimental conditions as reported above, except where the ammonia atmosphere was replaced by nitrogen were also performed. The results are primarily aligned carbon nanotubes and only small amounts of $B_xC_yN_z$ nanotubes. This suggests that N_2 is not efficient enough for the formation of high quality $B_xC_yN_z$ nanotubes at present low temperature. This shows that the formation of B–C–N bonds within the $B_xC_yN_z$ nanotubes from a NH_3 -containing gas phase at low temperature is feasible similar to the case in which NH_3 has proved efficient in the preparation of GaN nanorods¹⁹ and CN_x nanotubes.¹⁴ If the annealing time is increased (e.g., 1 h), the product has a more ordered structure, but the x/y ratio of $B_xC_yN_z$ nanotubes was unchanged.

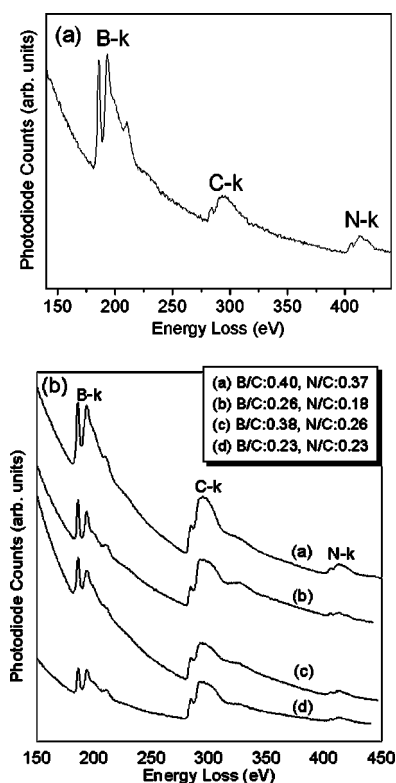


FIG. 3. (a) Typical EELS core electron K -shell spectrum taken from an individual nanotube of aligned $B_xC_yN_z$ nanotubes and (b) a comparison of EELS spectra recorded from four locations along the nanotube indicated in Fig. 2(a).

In a previous study of $B_xC_yN_z$ nanotubes synthesized by pyrolysis of $CH_3CN.BCl_3$ at ~ 900 – $1000^\circ C$ over Co powder,⁷ it was reported that the concentration of carbon at their tips was greater than in the rest of the length. It was suggested that carbon first agglomerates at the catalytic particle and that incorporation of boron and nitrogen into the sp^2 networks occurs subsequently.⁷ This prediction is not suitable for the present study. Our result shows that the incorporation of C, B, and N into the network of the nanotubes might be continuous through the entire growth.

The growth mechanism employed for the synthesis of aligned $B_xC_yN_z$ nanotubes by the present route is proposed with the following process. After the mixture of ferrocene, melamine, and B_2O_3 was moved to the high temperature zone of the first furnace from the cold zone, both ferrocene and melamine were sublimed at high temperature and were carried by the ammonia gas into the second furnace. Meanwhile, the boron oxide melted, as its melting point is about $450^\circ C$. Boron oxide vapor was carried by ammonia gas into the second furnace. Upon the decomposition of ferrocene, iron particles, surrounded by carbon, CN radicals, nitrogen and boron oxide, formed on the surface of quartz tube. Segregation of Fe then occurs, leading to an increase in the size of the catalytic center.²⁰ Once the Fe particle reaches an optimal size for nanotube nucleation,²¹ the surrounding carbon, nitrogen, and boron oxide transform into a $B_xC_yN_z$

nanotube. By blowing the mixture of ferrocene, melamine, and boron oxide into the furnace, the $B_xC_yN_z$ nanotubes grow continuously.

To summarize, uniform arrays of highly aligned $B_xC_yN_z$ nanotubes have been prepared by a new route, which consists of pyrolysis of organic reagents and vaporization of molten inorganic reagents. Using this route, aligned $B_xC_yN_z$ nanotubes might also be grown on other substrates. The heterogeneous composition within one $B_xC_yN_z$ nanotube implies that these aligned nanotubes might be used as aligned one dimension heterojunctions or superlattices, although how to precisely control the composition of the aligned $B_xC_yN_z$ nanotubes still remains a challenge.

The authors are grateful to C. Nelson, D. Ah Tye, and Dr. C. Kisielowski for help with SEM and TEM measurements. This research was supported in part by the Office of Energy Research, Office of Basic Energy Science, Division of Materials Sciences, U.S. Department of Energy (Contract No. DE-AC03-76SF00098) and NSF Grant No. DMR-9801738.

¹S. Iijima, *Nature (London)* **354**, 56 (1991).

²N. G. Chopra, R. J. Luyken, K. Cherrey, V. H. Crespi, M. L. Cohen, S. G. Louie, and A. Zettl, *Science* **269**, 966 (1995).

³X. Blase, J.-Ch. Charlier, A. De Vita, and R. Car, *Appl. Phys. A: Mater. Sci. Process.* **68**, 293 (1999).

⁴Ph. Redlich, J. Loeffler, P. M. Ajayan, J. Bill, F. Aldinger, and M. Rühle, *Chem. Phys. Lett.* **260**, 465 (1996).

⁵W. Han, Y. Bando, K. Kurashima, and T. Sato, *Appl. Phys. Lett.* **73**, 3085 (1998).

⁶K. Suenaga, C. Colliex, N. Demoncey, A. Loiseau, H. Pascard, and F. Willaime, *Science* **278**, 653 (1997).

⁷M. Terrones, A. M. Benito, C. Manteca-Diego, W. K. Hsu, O. I. Osman, J. P. Hare, D. G. Reid, H. Terrones, A. K. Cheetham, K. Prassides, H. W. Kroto, and D. R. W. Walton, *Chem. Phys. Lett.* **257**, 576 (1996).

⁸Y. Zhang, H. Gu, K. Suenaga, and S. Iijima, *Chem. Phys. Lett.* **279**, 264 (1997).

⁹W. Han, Y. Bando, K. Kurashima, and T. Sato, *Jpn. J. Appl. Phys., Part 1* **38**, 755 (1999).

¹⁰Y. Miyamoto, M. L. Cohen, and S. G. Louie, *Solid State Commun.* **102**, 605 (1997).

¹¹R. Sen, B. C. Satishkumar, A. Govindaraj, K. R. Harikumar, G. Raina, J. Zhang, A. K. Cheetham, and C. N. R. Rao, *Chem. Phys. Lett.* **287**, 671 (1998).

¹²K. Suenaga, M. P. Johansson, N. Hellgren, E. Broitman, L. R. Wallenberg, C. Colliex, J. E. Sundgren, and L. Hultman, *Chem. Phys. Lett.* **300**, 695 (1999).

¹³M. Terrones, H. Terrones, N. Grobert, W. K. Hsu, Y. Q. Zhu, J. P. Hare, H. W. Kroto, D. R. M. Walton, P. Redlich, M. Rühle, J. P. Zhang, and A. K. Cheetham, *Appl. Phys. Lett.* **75**, 3932 (1999).

¹⁴W. Han, Ph. Kohler-Redlich, T. Seeger, F. Ernst, M. Rühle, N. Grobert, W. K. Hsu, B. H. Chang, Y. Q. Zhu, H. W. Kroto, D. R. M. Walton, M. Terrones, and H. Terrones, *Appl. Phys. Lett.* **77**, 1807 (2000).

¹⁵K. B. Shelimov and M. Moskovits, *Chem. Phys.* **12**, 250 (2000).

¹⁶X. Bai, E. Wang, J. Yu, and H. Yang, *Appl. Phys. Lett.* **77**, 67 (2000).

¹⁷M. Terrones, N. Grobert, J. Olivares, J. P. Zhang, H. Terrones, K. Kordatos, H. K. Hsu, J. P. Hare, P. D. Townsend, K. Prassides, A. K. Cheetham, H. W. Kroto, and D. R. M. Walton, *Nature (London)* **388**, 52 (1997).

¹⁸C. N. R. Rao, R. Sen, B. C. Satishkumar, and J. Govindaraj, *J. Chem. Soc. Chem. Commun.* **15**, 1525 (1998).

¹⁹W. Han, S. Fan, Q. Li, and Y. Hu, *Science* **277**, 1287 (1997).

²⁰S. Huang, L. Dai, and A. W. H. Mau, *J. Phys. Chem. B* **103**, 4223 (1999).

²¹M. Yudasaka, R. Kikuchi, T. Matsui, Y. Ohki, and S. Yoshimura, *Appl. Phys. Lett.* **67**, 2477 (1995).